Cell Reports, Volume *36*

Supplemental information

Antibody:CD47 ratio regulates macrophage phagocytosis through competitive receptor phosphorylation

Emily C. Suter, Eva M. Schmid, Andrew R. Harris, Erik Voets, Brian Francica, and Daniel A. Fletcher

Supplemental Figure 1.

a

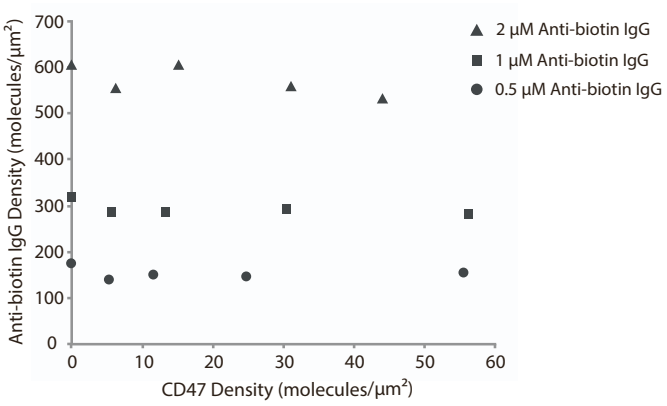

b

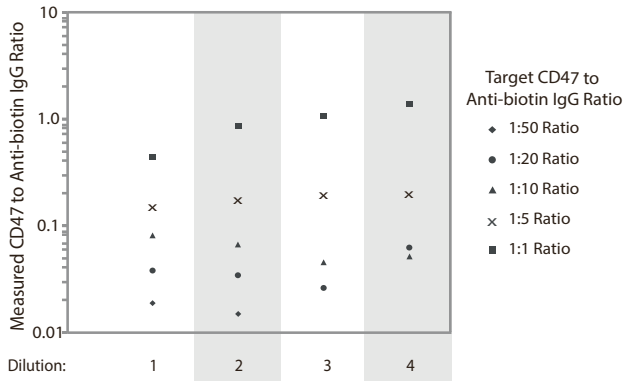

Figure S1. Quantification of bead surface densities of antibody and CD47. Related to Figure 1.

(a) Example target particle surface density data from phagocytosis assay summarized in Figure 1b. SLB-coated target particles were coated in different concentrations of AlexaFluor647-labeled anti-biotin IgG and AlexaFluor488-labeled CD47. Target particle fluorescence was measured via flow cytometry and compared to calibrated beads to calculate surface densities for each protein.

(b) Example target particle surface density data from phagocytosis assay summarized in Figure 1c. Target ratios of CD47 and anti-biotin IgG were created, then serially diluted 5-fold 3 times (for a total of 4 dilutions). Note that conditions that have no CD47 added or data points in which CD47 was diluted past detectable limits are not plotted.

Supplemental Figure 2.

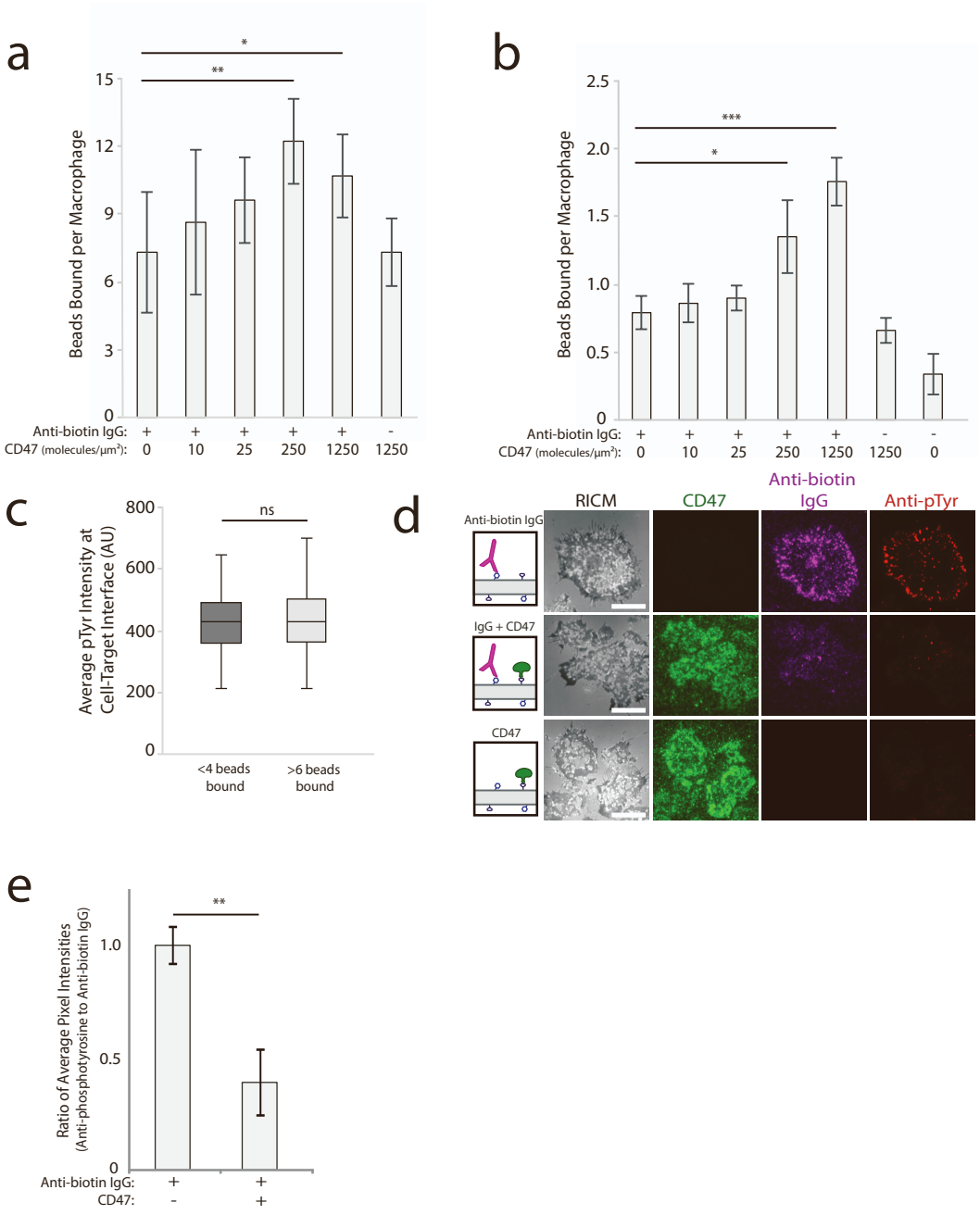

Figure S2. Measurement of binding and phosphorylation at immune interface. Related to Figures 2 and 3.

(a) Average number of beads bound to RAW 264.7 macrophages quantified in Figure 3a. Beads coated in anti-biotin IgG (300 molecules/μm^2) and CD47 (10-1250 molecules/μm^2) were incubated with macrophages for 10 minutes prior to fixation. Each condition is the average of 3 independent experiments representing a total of >40 cells. Bars represent mean ± s.e.m. Conditions were compared with two-tailed student's *t* test, with (*) denoting $p<0.05$ and (**) denoting $p<0.01$.

(b) Beads coated in anti-biotin IgG (300 molecules/μm^2) and CD47 (10-1250 molecules/μm^2) were incubated with RAW 264.7 macrophages at 4°C for 30 minutes to prevent phagocytosis, and bound beads were quantified. Each condition is the average of three independent experiments representing a total of >200 cells. Bars represent mean ± s.e.m. Conditions were compared with two-tailed student's *t* test, with (*) denoting $p<0.05$ and (***) denoting $p<0.001$.

(c) RAW 264.7 macrophages quantified in Figure 3a were partitioned into high engagement (>6 beads bound) and a low engagement (<4 beads bound) groups, and the average pTyr signal at bead interfaces was averaged for each group. Each condition represents >50 cell-target interfaces. Bars represent mean ± s.e.m. Conditions were compared with two-tailed student's *t* test, with (**) denoting $p<0.01$.

(d) RAW 264.7 macrophages were dropped onto SLBs coated in AlexaFluor647-labeled anti-biotin IgG (magenta), AlexaFluor488-labeled CD47 (green), or both. Cells were imaged using RICM and TIRF microscopy. Scale bar is 5 μm.

(e) The fluorescence ratio of anti-phosphotyrosine to anti-biotin IgG was quantified for each footprint. Each condition is the average of >50 footprints. Bars represent mean ± s.e.m. Conditions were compared with two-tailed student's *t* test, with (**) denoting $p<0.01$.

Supplemental Figure 3.

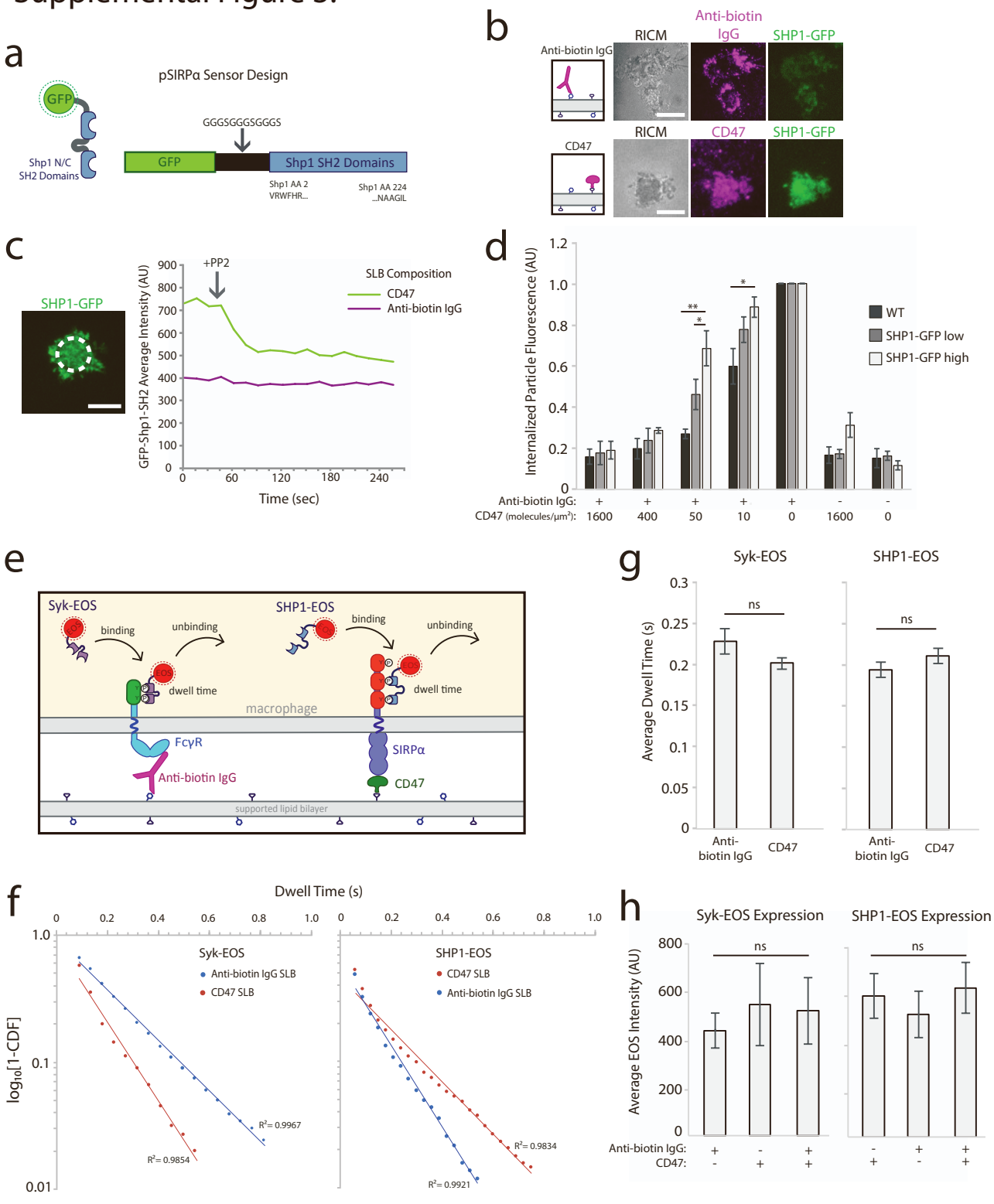

Figure S3. Design and measurement of phosphorylation sensors. Related to Figure 3.

(a) Design of SHP1-GFP sensor for phosphorylated SIRPα. GFP was linked to the tandem SH2 domains of SHP1, which bind to phosphorylated ITIMs in the cytoplasmic tail of SIRPα.

(b) Representative TIRF and RICM images of RAW 264.7 cells expressing SHP1-GFP (green) on SLBs containing either anti-biotin IgG only or CD47 only (each labeled with AlexaFluor647, magenta). Scale bar is 10 μm.

(c) Effect of addition of 1μM Src family kinase inhibitor PP2 on SHP1-GFP sensor intensity. Src family kinase Lyn is responsible for phosphorylation of SIRPα, and decreasing SIRPα phosphorylation prevents SHP1 binding. Sensor intensity over time was measured in region indicated by white circle. Scale bar is 10 μm.

(d) Phagocytosis was quantified for target particles with a range of CD47:antibody densities with RAW 264.7 macrophages stably expressing SHP1-GFP at high or low levels. Each condition is the average of three independent experiments representing a total of >300 cells. Bars represent mean ± s.e.m. Conditions were compared with two-tailed student's *t* test, with (*) denoting $p<0.05$ and (**) denoting $p<0.01$.

(e) Binding of Syk-EOS and SHP1-EOS to their preferred targets, phosphorylated FcγR and SIRPα, respectively. Binding events and molecule dwell times were quantified from TIRF timelapse images.

(f) Cumulative distribution function for SHP1-EOS (left) and Syk-EOS (right) dwell times. RAW 264.7 cells stably expressing SHP1-EOS and Syk-EOS were dropped onto SLBs coated in either anti-biotin IgG (300 molecules/μm^2) or CD47 (500 molecules/μm^2).

(g) Average dwell time for Syk-EOS and SHP1-EOS was quantified from binding event dwell times quantified in Figure S3e. Each condition is the average of three independent experiments representing a total of >3000 binding events per condition. Bars represent mean ± s.e.m. Conditions were compared with two-tailed student's *t* test.

(h) SHP1-EOS and Syk-EOS expression of cells quantified in Figure 3d. Expression was assessed by quantifying average GFP intensity in cell footprint. Each condition is the average of 3 independent experiments representing a total of >50 macrophage footprints. Bars represent mean ± s.e.m. Conditions were compared with one-way ANOVA statistical test.

Supplemental Figure 4.

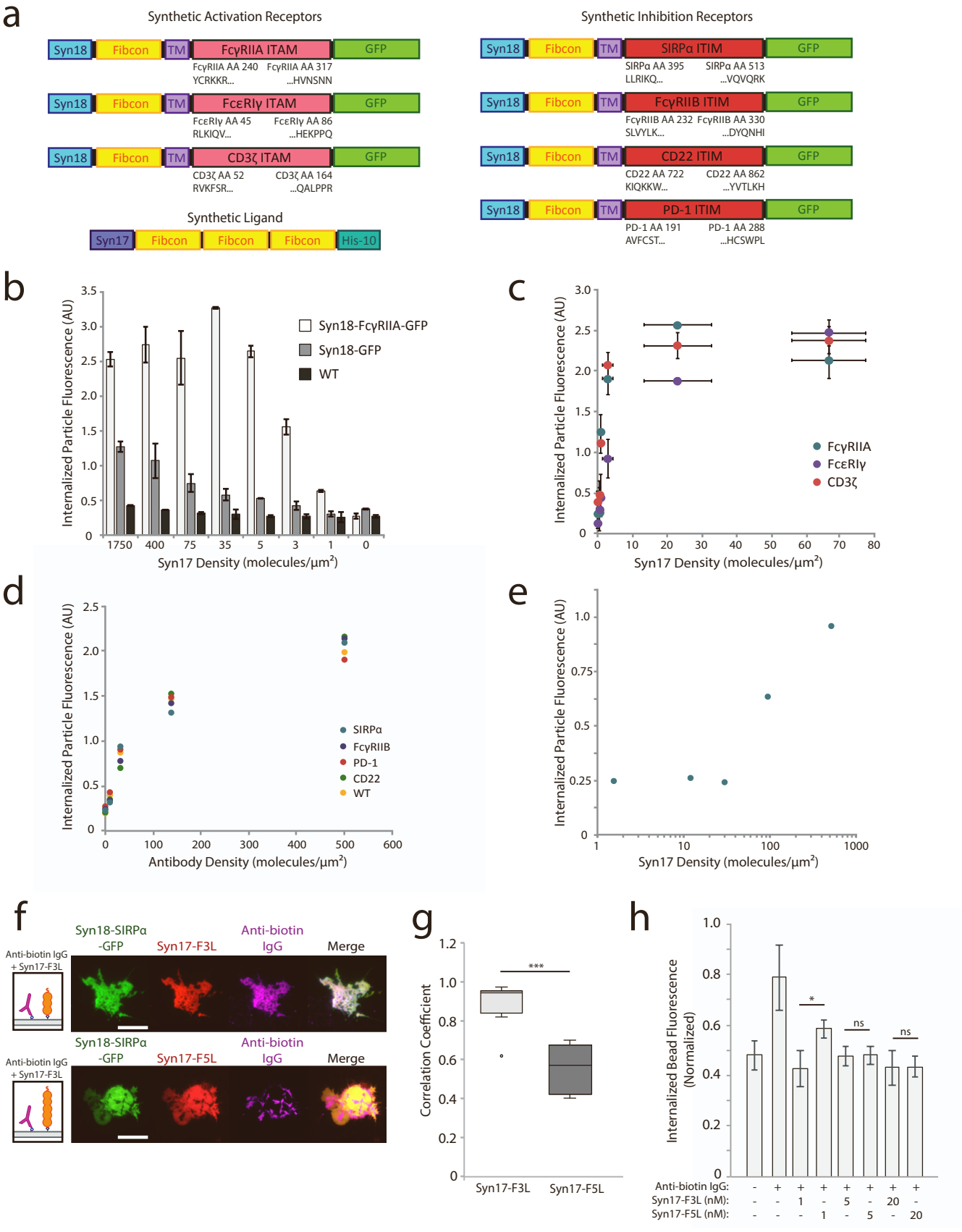

Figure S4. Validation of ITAM- or ITIM-containing synthetic receptors. Related to Figure 4.

(a) Schematic of synthetic chimeric receptor constructs. Synthetic activation receptors signaled via FcγRIIA, FcεRI γ-chain, and CD3 ζ-chain ITAM-containing intracellular domains. Synthetic inhibition receptors signaled via FcγRIIB, PD-1, SIRPα, and CD22 ITIM-containing intracellular domains.

(b) Target particles with varying surface densities of Syn17-F3L (0-1750 molecules/μm^2) were incubated with RAW 264.7 macrophages stably expressing Syn18-FcγRIIA-GFP receptor (light gray bars) and non-signaling Syn18-GFP (medium gray bars), as well as wild type macrophages (WT, dark gray bars). Average phagocytosis was quantified. Each condition is the average of three independent experiments representing a total of >300 cells. Bars represent mean ± s.e.m.

(c) Phagocytosis of Syn17-3L-coated target particles with macrophages expressing different Syn18 activating receptors. RAW 264.7 macrophages independently express Syn18 receptors containing FcγRIIA, FcεRI γ-chain, and CD3 ζ-chain intracellular signaling motifs. Target particles coated with increasing Syn17-F3L densities (0-75 molecules/μm^2) were simultaneously added to each receptor cell line, and average phagocytosis was quantified in the absence of an inhibitory ligand. Each condition is the average of three independent experiments representing a total of >300 cells. Dots represent mean ± s.e.m.

(d) Phagocytosis of anti-biotin IgG coated target particles by macrophages expressing different Syn18 inhibitory receptors. RAW 264.7 macrophages independently express Syn18 receptors containing FcγRIIB, PD-1, SIRPα, and CD22 intracellular signaling motifs. Target particles coated with increasing anti-biotin IgG surface densities (0-500 molecules/ μm^2) were simultaneously added to each receptor cell line as well as WT macrophages, and average phagocytosis was quantified in the absence of an inhibitory ligand. Each condition is the average of >100 cells.

(e) Phagocytosis of Syn17-F3L coated target particles by macrophages expressing Syn18-SIRPα-GFP. Phagocytosis was quantified for target particles coated in increasing densities of Syn17-F3L (0-500 molecules/μm^2) in the absence of an activating ligand. Each condition is the average of >100 cells.

(f) Representative TIRF images of RAW 264.7 cells expressing Syn18-SIRPα-GFP (green) on SLBs containing anti-biotin IgG (magenta) plus either Syn17-F3L or Syn17-F5L (red). Scale bar is 10 μm.

(g) Pearson's correlation coefficient comparing anti-biotin IgG localization with either Syn17-F3L or Syn17-F5L. Conditions were compared with two-tailed student's *t* test, with (***) denoting $p<0.001$.

(h) Phagocytosis of target particles coated in anti-biotin IgG and different concentrations of Syn17 ligand was quantified for Syn18-SIRPα-GFP macrophages. Phagocytosis levels of Syn18-SIRPα-GFP expressing cells were normalized to non-signaling Syn18-GFP expressing cells to account for the impact of increased steric bulk of the Syn17-F5L on anti-biotin IgG accessibility. Each condition is the average of three independent experiments representing a total of >300 cells. Bars represent mean ± s.e.m. Conditions were compared with two-tailed student's *t* test, with (*) denoting $p<0.05$.

Supplemental Figure 5.

a

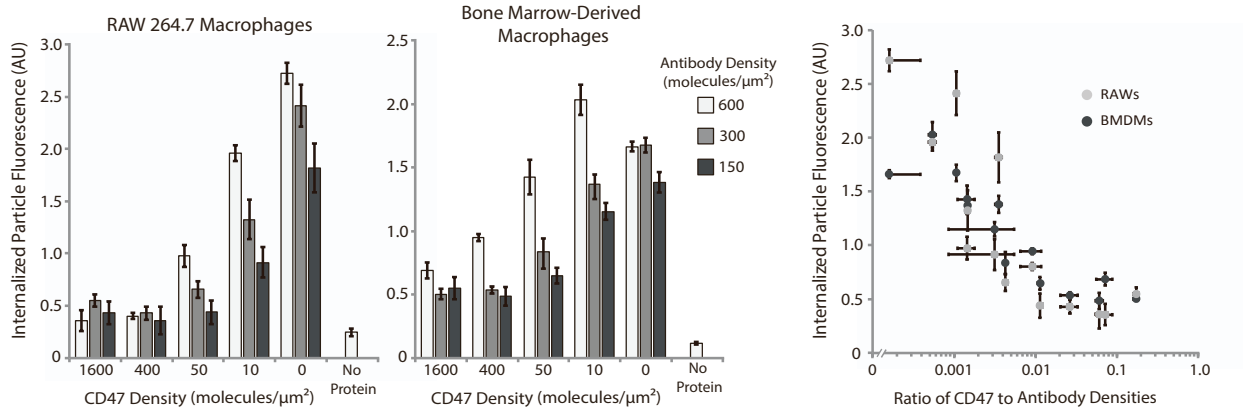

b

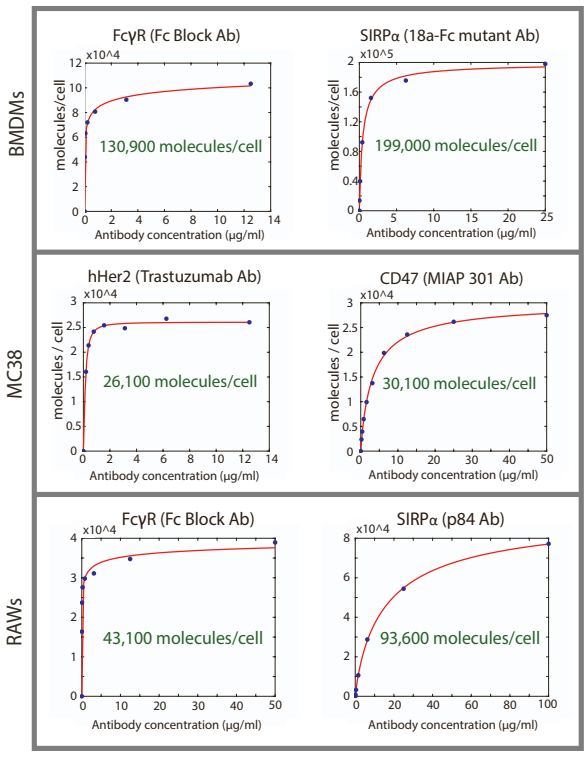

Figure S5. Characterization of BMDM phagocytosis and cell surface densities. Related to Figure 5.

(a) Phagocytosis comparison between RAW 264.7 macrophages and BMDMs. To create a panel of target particle compositions, three different anti-biotin IgG surface densities (150, 300, 600 molecules/μm^2) were combined with five different CD47 densities (0-1600 molecules/μm^2), plus an additional no protein (lipid only) control. All 16 different target particle densities were simultaneously added to RAWs and BMDMs, and average phagocytosis was quantified (left and center panels). Data replotted as a function of CD47:antibody ratio (right panel). Each condition is an average of 3 independent experiments representing >200 total cells. Bars represent mean ± s.e.m.

(b) Measurements of surface densities on RAW 264.7 macrophages, BMDMs, and MC38-hHER2 tumor cells. AlexaFluor647-labeled antibodies for FcγRs (Fc Block), SIRPα (18a Fc mutant and p84), hHER2 (anti-hHER2), and CD47 (MIAP 301) were increased to receptor saturating concentrations and measured via flow cytometry. Number of molecules per cell was estimated by fitting a Hill equation to each antibody titration and calculating y_{max}.

Supplemental Table 1.

Equations implemented in interacting kinetic model
(p denotes phosphorylated state)

$$\frac{\partial}{\partial t}[FcR] = -k_1[Ab][FcR] + k_2[FcR - Ab]$$

$$\frac{\partial}{\partial t}[FcR - Ab] = k_1[Ab][FcR] - k_2[FcR - Ab] - k_3[FcR - Ab] + k_{13}[SIRP\alpha - Shp1 - FcR_p]$$

$$\frac{\partial}{\partial t}[Ab] = -k_1[Ab][FcR] + k_2[FcR - Ab]$$

$$\frac{\partial}{\partial t}[FcR_p] = k_3[FcR - Ab] - k_4[FcR_p][Syk] + k_5[FcR - Syk] - k_{11}[SIRP\alpha - Shp1][FcR_p] + k_{12}[SIRP\alpha - Shp1 - FcR_p]$$

$$\frac{\partial}{\partial t}[FcR - Syk] = k_4[FcR_p][Syk] - k_5[FcR - Syk]$$

$$\frac{\partial}{\partial t}[Syk] = -k_4[FcR_p][Syk] + k_5[FcR - Syk]$$

$$\frac{\partial}{\partial t}[SIRP\alpha] = -k_6[SIRP\alpha][CD47] + k_7[SIRP\alpha - CD47]$$

$$\frac{\partial}{\partial t}[CD47] = -k_6[SIRP\alpha][CD47] + k_7[SIRP\alpha - CD47]$$

$$\frac{\partial}{\partial t}[SIRP\alpha - CD47] = k_6[SIRP\alpha][CD47] - k_7[SIRP\alpha - CD47] - k_8[SIRP\alpha - CD47]$$

$$\frac{\partial}{\partial t}[SIRP\alpha_p] = k_8[SIRP\alpha - CD47] - k_9[SIRP\alpha_p][Shp1] + k_{10}[SIRP\alpha - Shp1]$$

$$\frac{\partial}{\partial t}[SIRP\alpha - Shp1] = k_9[SIRP\alpha_p][Shp1] - k_{10}[SIRP\alpha - Shp1] - k_{11}[SIRP\alpha - Shp1][FcR_p] + k_{12}[SIRP\alpha - Shp1 - FcR_p] + k_{13}[SIRP\alpha - Shp1 - FcR_p]$$

$$\frac{\partial}{\partial t}[Shp1] = -k_9[Shp1][SIRP\alpha_p] + k_{10}[SIRP\alpha - Shp1]$$

$$\frac{\partial}{\partial t}[SIRP\alpha - Shp1 - FcR_p] = k_{11}[SIRP\alpha - Shp1][FcR_p] - k_{12}[SIRP\alpha - Shp1 - FcR_p] - k_{13}[SIRP\alpha - Shp1 - FcR_p]$$

Table S1. Differential equations implemented for interacting kinetic model. Related to Figure 3.

Equations were simulated in Python 3.5.

Supplemental Table 2.

Rate Constant	Value	Citation	Notes
k_1	8.2×10^3 $M^{-1}s^{-1}$	Li et al, 2007	
k_2	5.7×10^{-3} s^{-1}	Li et al, 2007	
k_3	0.15 s^{-1}	Barua et al, 2012	Estimated from value for unphosphorylated Lyn
k_4	1.8×10^5 $M^{-1}s^{-1}$	Barua et al, 2012	
k_5	0.3 s^{-1}	Barua et al, 2012	
k_6	2×10^5 $M^{-1}s^{-1}$	Brooke et al, 2004	
k_7	5.3 s^{-1}	Brooke et al, 2004	
k_8	0.15 s^{-1}	Barua et al, 2012	Same as k_3; Assumes no ITAM vs. ITIM preference
k_9	1.8×10^6 $M^{-1}s^{-1}$	Barua et al, 2012	Estimate from other SFKs
k_{10}	0.1 s^{-1}	Barua et al, 2012	
k_{11}	1.8×10^5 $M^{-1}s^{-1}$	Ren et al, 2011	Estimated from k_d value
k_{12}	5 s^{-1}	Ren et al, 2011	
k_{13}	66 s^{-1}	Selner et al, 2014	Measured value for peptide w/I at Y -2 position

Table S2. Rate constants utilized in phagocytosis kinetic model. Related to Figure 3.

Constants that were estimated from published values are noted.